



Sandpile under rotational constraint

S B Santra* and D Deb

Department of Physics, Indian Institute of Technology Guwahati,
Guwahati-781 039, Assam, India

E-mail santra@iitg.ernet.in

Abstract Sandpile model is studied here imposing rotational constraint on the flow of sand grains. The rotational constraint is constituted by certain deterministic rules. The rotational dynamics evolves the system into a non-equilibrium steady state characterized by power law correlations and exhibits self organized criticality. The exponents characterizing the power law distributions of avalanche properties are found different from other models. Consequently the present model belongs to a new universality class.

Keywords Sandpile, self-organized criticality, rotational constraint

PACS Nos. 45.70.Cc, 05.65.+b

1. Introduction

The phenomenon that a class of externally driven systems evolves naturally into a state of no single characteristic size or time is known as self-organized criticality (SOC) [1]. The non-equilibrium steady state in SOC is characterized by long range spatio-temporal correlations and power law scaling behavior. SOC was established for the first time through sandpile model by Bak, Tang and Wiesenfeld (BTW) [2]. Sandpile then became a prototypical model for studying SOC. The model was studied widely and many results are available in the literature [3]. A variant of BTW model is Manna's stochastic model (MSM) [4]. In MSM, sand grains flow in randomly selected directions rather than in all possible direction on a lattice as in BTW. Extensive attention has also been paid to MSM. It was a controversial issue over a period of time whether MSM belong to the same universality class of BTW or not [5]. In MSM, the distribution functions of avalanche properties obey finite size scaling (FSS) whereas in BTW, some of them obey multi-scaling rather than FSS. Recently, it has been concluded that MSM belongs to a different universality class than that of BTW from moment analysis of the avalanche distribution functions [6-8].

In this paper, a new two state sandpile model is constructed imposing rotational constraint on the flow of sand grains. In this rotational sandpile model (RSM), the toppling rules are deterministic except at the very first toppling. A site topple if it exceeds the predefined critical height and two sand grains flow in the forward direction or in a specific rotational direction, say clockwise. A physical realization of RSM could be a sandpile on a rotating disk where the disk is rotating about an axis perpendicular to the plane of the disk and passing through the center of the disk. It is found that the rotational dynamics adopted here evolves the system into a non-equilibrium steady state at which the average height of the sandpile remains constant. The spatio-temporal correlations in the non-equilibrium steady state of RSM are characterized by power law distributions.

2. Rotational sandpile model

RSM is defined here on a square lattice in two dimensions (2D). A positive integer h_i is assigned to each lattice site, called the height of the site. Initially, all the h_i s are set to zero. Sand grains are added to randomly chosen lattice sites and the variable h_i is incremented to $h_i + 1$ if a sand grain is added to the i th site. A site is called active when the height of a site becomes greater than or equal to a predefined threshold value $h_c = 2$, as in MSM. Toppling of the first active site initiates an avalanche. This site can be called the origin of the avalanche. On the very first toppling of the active site, two sand grains are given away to two randomly selected nearest neighbors out of four nearest neighbors on a square lattice. As soon as a site receives a sand grain, the direction d_i from which the grain was received is assigned to it along with the increment of its height h_i . The value of d_i can change from 1 to 4 as there are four possible directions on the square lattice. As the avalanche propagates, the direction d_i and height h_i are updated on receiving a sand grain and only the information from which direction the last sand grain was received is kept. The next active site with $h_i > 2$ in the avalanche will topple and two sand grains will flow in the direction from which the last grain was received and to a clockwise rotational direction. The toppling rules can be stated as

$$h_i \rightarrow h_i - 2$$

$$h_j \rightarrow h_j + 1, \quad j = d_i \text{ \& \ } d_i + 1 \quad (1)$$

where d_i is the direction from which the last sand grain was received by the i th site. If j becomes greater than 4 it is taken to be 1. Toppling of active sites are then made deterministically in this model except at the origin. The propagation of the avalanche stops if all sites in the lattice become under critical. The duration or lifetime of an avalanche is taken as the number of parallel updates to make all the sites under critical. The avalanche dynamics is studied with the open boundary condition. During an avalanche no sand grain is added. The steady state of this dynamical system corresponds to the constant average height of the sandpile.

A typical avalanche obtained in the steady state of RSM on a square lattice of size $L = 128$ is shown in Figure 1. The grey level of a site depends on the number of times it has toppled. It is found here that the number of toppling of a single active site varies from 1 to the order of lattice size L . In Figure 1, bright grey level corresponds to the maximum number of toppling and dark grey level corresponds to the minimum number of toppling



Figure 1. A typical RSM avalanche generated on a square lattice of size 128×128 is shown. The grey level of a site depends on the number of times it has toppled. Low grey level corresponds to the maximum number of toppling and high grey level corresponds to the minimum number of toppling, i.e. one. White space inside the avalanche corresponds to the sites that did not topple at all during the avalanche. The area of the avalanche is 12256, total number of toppling is 211992 and the maximum number of toppling of a site is 68.

White space inside the avalanche corresponds to the sites that did not topple at all during the avalanche. It can be seen that there are more than one bright spots along with mixing of grey levels. The occurrence of several bright spots and mixing of grey levels indicates that there are several regions of higher number of toppling surrounded by regions of lower number of toppling. The regions of lower number of toppling may exist inside the region of higher number of toppling. This is unusual in BTW model [9]. However, this happens in MSM since sand flows stochastically [4]. This is demonstrated for both BTW and MSM by Ben-Hur and Biham [5]. It can also be noticed that there are several white space or holes (no toppling region) inside the avalanche. In BTW, the avalanches are compact and do not include any hole inside avalanche [9]. However, there exist some holes inside the avalanche in Manna's directed model [10]. Thus, the avalanche cluster is similar to that of MSM even though the toppling rules are deterministic here in RSM. The final state in an avalanche will depend on the sequence of toppling due to the deterministic rules considered here. Consequently, the model is nonabelian like MSM.

RSM is thus a new two state deterministic nonabelian sandpile model. It is then interesting to characterize the avalanche properties of RSM at its non-equilibrium steady

state. Below, the steady state of RSM is characterized by calculating the probability distributions of avalanche properties.

3. Results and discussion

The non-equilibrium steady state is defined by the constant average height of the sandpile at which the rate of influx of sand grain to the system is equal to the rate of out flux at the open boundary. In order to identify the steady state the average height

$$\langle h \rangle = \frac{1}{L^2} \sum_i^L h_i \tag{2}$$

has been measured generating 10^6 avalanches. The average height $\langle h \rangle$ is plotted against the number of avalanches in Figure 2 for $L = 2048$. It can be seen that a constant average height is obtained. The value of $\langle h \rangle$ remains constant over a large number of avalanches. For smaller lattice sizes the steady states are reached by smaller number of avalanches. A slight variation of the average height with the system size is observed. The values of $\langle h \rangle$ against the system size are shown in the inset. In order to characterize the physical properties of the avalanches occurred at the steady, simulations have been performed on the square lattice of sizes $L = 128$ to $L = 2048$ in multiple of 2. First 10^5 avalanches were skipped to achieve the steady state. Extensive data collection have made for each lattice size for averaging, ranging from 32×10^6 avalanches for $L = 128$ down to 2×10^6 avalanches for $L = 2048$ in ten configurations. In each configuration the initial 10^5 avalanches are neglected again at the steady state before collecting data.

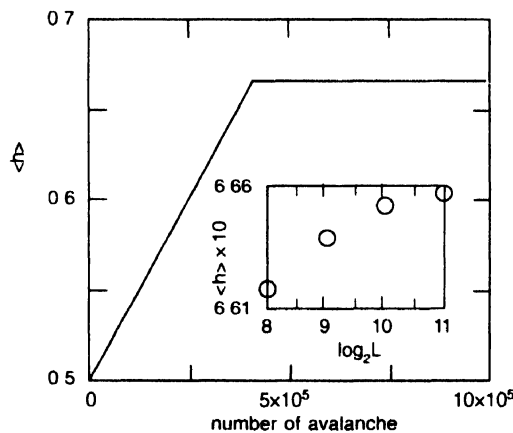


Figure 2. Plot of average height $\langle h \rangle$ against the number of avalanches. The value of $\langle h \rangle$ remains constant over a large number of avalanches and changes slightly with the system size L . Dependence of $\langle h \rangle$ on the system size L is shown in the inset.

The characterization of the physical properties of the avalanches occurred at the steady state are made by measuring : the total number of toppling s , the area a of the avalanche, the lifetime t of an avalanche and the spatial extension of the avalanche l . The probability

distributions of all these properties (s, a, t, l) are determined. The probability distribution functions of the avalanche related quantities at the steady state are expected to obey power law behavior

$$P(x) \tag{3}$$

where τ_x is the corresponding critical exponent and x stands for s, a, t and l . Data are collected in bins of 10s, 100s, 1000s and so on and finally it is normalized by bin widths. In Figure 3, the probability distribution $P(x)$ is plotted against x where x corresponds to toppling numbers s (diamonds), area a (circles), life time t (triangles) and spatial extension l (squares). It can be seen that the distributions $P(x)$ follow reasonable power law behavior for each property x . The values of the associated critical exponents τ_x are obtained as $\tau_s = 1.224 \pm 0.003$, $\tau_a = 1.334 \pm 0.004$, $\tau_t = 1.389 \pm 0.005$ and $\tau_l = 1.667 \pm 0.005$. The error bars quoted here are the least square fitting errors taking into account of statistical error of each data point. In the inset of Figure 3, the distribution of scaling numbers $P(s)$ are plotted against s for different lattice sizes. It can be seen that the same power law behavior is obtained for all the system sizes L . The slope obtained for different L is within the error bar already mentioned with the respective exponents. The values of the exponents for BTW are $\tau_s \approx 1.293$, $\tau_a \approx 1.330$, $\tau_t \approx 1.480$ and $\tau_l \approx 1.665$ and for MSM they are $\tau_s \approx 1.275$, $\tau_a \approx 1.373$, $\tau_t \approx 1.493$ and $\tau_l \approx 1.743$. The values of the exponents for BTW and MSM taken from Ref [5,11,12]. Interestingly, the toppling number exponent τ_s and the lifetime exponent τ_t are only slightly different from that of BTW whereas τ_a and τ_l are almost the same. The disagreement of the lifetime and toppling distribution exponents with that of the BTW exponents can be accounted by the fact that in RSM the avalanche waves generally have a spiraling nature around some regions within the avalanche cluster and as a consequence it will take longer time and large number of topplings for an

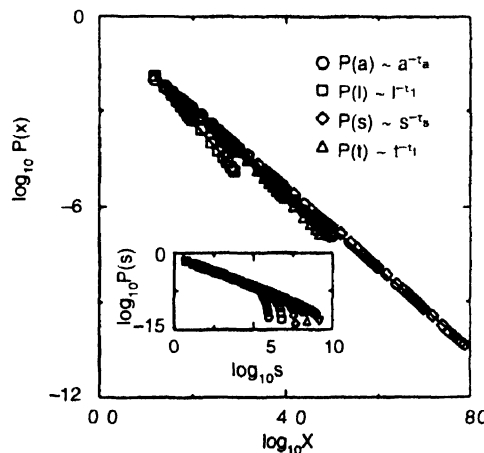


Figure 3. Plot of probability distributions of number of toppling in an avalanche $P(s)$ (\diamond), avalanche area $P(a)$ (\circ), lifetime $P(t)$ (Δ) and extension of avalanche $P(l)$ (\square) against the corresponding variables s, a, t and l . Reasonable power law distributions are obtained for all the properties. In the inset, $P(s)$ is plotted against s for different system size L .

avalanche to die away than that in BTW. On the other hand, in comparison to MSM most of the exponents are found different. Note that $\tau_s = 2 - 1/\tau_a$, conjectured by Majumder and Dhar [13], is satisfied by in case of MSM The conjecture is found not valid for BTW It can be seen that the conjecture is also not valid in case of RSM. The expected value of τ_s in RSM form the conjecture is ≈ 1.25 outside the error bar of the obtained value 1.224 ± 0.003 . Thus, from the point of power law correlations, the avalanche properties are close to that of BTW and different from MSM.

Since the avalanche properties are related to each other, conditional expectation values can be defined. The conditional expectation value of an avalanche property x when another property is exactly equal to y is defined as

$$\langle x(y) \rangle = \sum xP(x,y) \tag{4}$$

where $P(x,y)$ is the probability to find a property x when the other property is exactly equal to y . It is expected that the expectation values will scale with its argument as

$$\langle x(y) \rangle \sim y^{\gamma_{xy}} . \tag{5}$$

Four expectation values $\langle s(a) \rangle \sim a^{\gamma_{sa}}$, $\langle a(t) \rangle \sim t^{\gamma_{at}}$, $\langle a(l) \rangle \sim l^{\gamma_{al}}$ and $t(l) \sim l^{\gamma_{tl}}$ are calculated on a square lattice of size $L = 2048$ and their scaling behavior are determined In Figure 4, the expectation values are plotted against their arguments in order to evaluate the exponents γ_{xy} . From the best fitted straight lines the estimated values of the exponents are $\gamma_{sa} = 1.453 \pm 0.003$, $\gamma_{at} = 1.167 \pm 0.005$, $\gamma_{al} = 2.002 \pm 0.002$ and $\gamma_{tl} = 1.715 \pm 0.005$ The values of the exponents for BTW are $\gamma_{sa} \approx 1.06$, $\gamma_{at} \approx 1.53$, $\gamma_{al} \approx 2$ and $\gamma_{tl} \approx 1.32$ and for MSM they are : $\gamma_{sa} \approx 1.23$, $\gamma_{at} \approx 1.35$, $\gamma_{al} \approx 2$ and $\gamma_{tl} \approx 1.49$ The

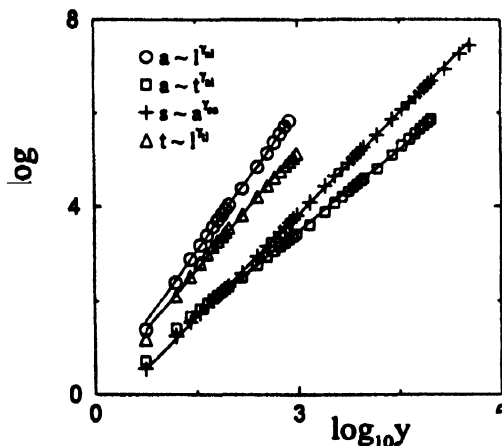


Figure 4. Plot of inter dependence of avalanche properties toppling (s) versus area (a) (+), area (a) versus extension (l) (O), area (a) versus time (t) (□) and time (t) versus length (l) (Δ) The solid line shows the best fitted straight line part

values of the exponents for BTW and MSM are taken from the Ref. [5,11,12]. There are few things to notice. First, γ_{sa} is found greater than one and a relevant exponent. This is expected because in this model, a site topples many times in an avalanche due to rotational constraint. Second, the exponent γ_{al} is found ≈ 2 since the avalanches are almost compact with a very few holes here and there. This is also the case for other models. Third, the value of the dynamical exponent γ_H is the highest in RSM and it is lowest in BTW. Since $\gamma_{xy} = 1/\gamma_{yx}$, the inverse of the dynamical exponent is γ_H which describes the diffusion of sand grains with respect to time. In that case, diffusion will be slowest in RSM and it will be fastest in BTW. This is expected. Because, the rotational constraint takes the sand grains into the interior of the system. Fourth, according to the scaling form given in eq. 5, the exponents should satisfy the scaling relation $\gamma_{xz} = \gamma_{xy}\gamma_{yz}$. It can be seen that the scaling relation $\gamma_{al} = \gamma_{at}\gamma_H$ is satisfied within error bars. Fifth, the values of γ_{sa} , γ_{at} and γ_H are found different from that of BTW as well as MSM except γ_{al} . Finally, a set of scaling relations between the distribution exponents τ_x and the exponents γ_{xy} describing the conditional expectation values of the avalanche properties can be obtained from the following identity

$$\int \langle x(y) \rangle P(y) dy = \int \langle x(z) \rangle P(z) dz \quad (6)$$

which would be satisfied by any set of three stochastic variables x , y and z . Using this identity and the relation $\gamma_{xz} = \gamma_{xy}\gamma_{yz}$, the following scaling relation can be obtained

$$\gamma_{xy} = (\gamma_y - 1) / (\gamma_x - 1). \quad (7)$$

The above scaling relations for $x, y \in \{s, a, l, t\}$ are satisfied within error bars for the numerical values obtained here. Thus, the exponents obtained here in RSM are consistent with the scaling relations but different from that of the BTW as well as MSM. It indicates that RSM belongs to a new universality class. In a recent study, Biham *et al* [14] showed a crossover behavior of critical exponents from Zhang model [15] to that of BTW model [2] depending upon a non-universal parameter p , the probability of sand flow in a given direction.

Following Karmakar *et al* [10], moment analysis of avalanche properties, $\langle x^q \rangle = \int x^q P(x, L) dx \approx L^{\sigma_x(q)}$, have been performed. It is found that RSM follows finite size scaling like MSM rather than multi scaling like BTW. This observation is also supported by the negative time autocorrelation of toppling waves constituting avalanche.

4. Conclusion

A new two state deterministic sandpile model. RSM, is defined imposing rotational constraint on the original BTW model. The non-equilibrium steady state of RSM is characterized by power law distribution of avalanche properties and exhibits SOC. The exponents describing

the power laws are found close to that of BTW. The values of the exponents satisfy the scaling relations among them within error bars. The rotational sandpile model therefore does not belong either in BTW or in MSM. RSM then belongs to a new universality class.

Acknowledgment

This work is financially supported by BRNS, DAE, India, grant no. 2005/37/5/BRNS.

References

- [1] H J Jensen *Self-Organized Criticality* (Cambridge) (1998)
- [2] P Bak, C Tang and K Wiesenfeld *Phys. Rev. Lett* **59** 381 (1987)
- [3] D Dhar *Physica* **A263** 4 (1999) and references therein.
- [4] S S Manna *J. Phys. A · Math. Gen* **24** L363 (1991) ; *Physica* **A179** 249 (1991)
- [5] A Ben-Hur and O Biham *Phys. Rev.* **E53** R1317 (1996)
- [6] C Tebaldi, M De Menech and A L Stella *Phys. Rev. Lett.* **83** 3952 (1999)
- [7] S Lübeck *Phys. Rev.* **E61** 204 (2000)
- [8] R Karmakar and S S Manna *Phys. Rev.* **E71** R015101 (2005)
- [9] P Grassberger and S S Manna *J. Phys. (Paris)* **51** 1077 (1990); S Banerjee, S B Santra and Bose *Z. Phys.* **B96** 571 (1995)
- [10] R Karmakar, S S Manna and A Stella *Phys. Rev. Lett* **94** 088002 (2005)
- [11] S Lübeck and K D Usadel *Phys. Rev.* **E55** 4095 (1997)
- [12] A Chessa, H E Stanley, A Vespignani and S Zapperi *Phys. Rev.* **E59** R12 (1999)
- [13] S N Majumder and D Dhar *Physica* **A185** 129 (1992)
- [14] O Biham, E Milshtein and O Malcai *Phys. Rev.* **E63** 061309 (2001)
- [15] Y C Zhang *Phys. Rev. Lett* **63** 470 (1989)